Int. J. Heat Mass Transfer. Vol. 19, pp. 635–641. Pergamon Press 1976. Printed in Great Britain

MASS-TRANSFER KINETICS IN DISSOLVING POLYDISPERSE SOLID MATERIALS

P. DITL, J. ŠESTÁK and K. PARTYK
ČVUT—Faculty of Mechanical Engineering, Suchbátarova 4, 166 07 Prague 6, Czechoslovakia

(*Received* 23 *December* 1974)

Abstract—A theoretical model for the dissolution of polydisperse mixtures of solid particles in mechanically agitated liquids has been developed. Results of the theoretical analysis are presented in terms of expressions in which the mass of the solid solute time rate of mass transfer and the particle size distribution explicitly depend on time. The general equations given in the paper are valid regardless of the particular form of the size distribution function. As an example, the general equations are integrated for the special case of the Rosin, Rammler and Sperling (RRS) distribution. Results of the analysis are presented in the form of graphical relations between dimensionless quantities. In order to verify the results obtained theoretically, experiments were carried out in which polydisperse mixtures of potassium sulfate particles were dissolved in distilled water. Very good agreement between theory and experiment has been observed.

NOMENCLATURE

A,	interphase surface;
c,	concentration;
c_s,	concentration of the saturated solution;
D,	vessel inner diameter;
$I(\vartheta, m)$,	function defined in equation (36) and tabulated in [8];
k,	mass-transfer coefficient;
M,	total mass of the polydisperse mixture;
M_p,	mass of a single particle;
$\dot{M}$,	time rate of mass transfer, equation (15);
n_p,	particle number;
n,	polydispersity index;
p,	size frequency distribution;
R,	cumulative oversize (residue) distribution;
t,	physical time;
W,	mass-transfer characteristic defined in equation (20);
x,	characteristic linear dimension of particle;
$\dot{x}$,	time rate of particle size change;
$\bar{x}$,	mean statistical particle size in the RRS-distribution.

Greek symbols

$\Gamma(\vartheta, m)$,	incomplete gamma function defined in equation (35);
$\Gamma(m)$,	gamma function;
η,	dimensionless particle size defined in equation (31);
ϑ,	dimensionless time defined in equation (28);
ξ,	dimensionless particle size defined in equation (26);
ρ_s,	density of the solid particle;
σ,	sphericity;
τ,	dimensionless time defined in equation (30);
ψ,	function of time defined in equation (14).

Other symbols

Δc,	$= c_s - c$, concentration difference.

Superscript

(x),	refers to particles in the size range x to $x + \mathrm{d}x$.

Subscripts

0,	initial value, $t = 0$;
max,	maximum value;
min,	minimum value.

1. INTRODUCTION

MOST studies dealing with heat- or mass-transfer problems in solid–fluid heterogeneous systems published so far were carried out for either a single solid particle or for monodisperse mixtures of solid particles. Since the majority of real mixtures is in fact of a polydisperse nature, the theoretical description of the heat- or mass-transfer process across the solid–fluid boundary is of interest in various fields of process engineering. Particular cases of mass transfer across the interphase boundary may be classified, e.g. according to whether the particle size increases during the process (e.g. crystallization [12], chemical reactions [13]) or whether a gradual particle size decrease is encountered (dissolution, combustion, disintegration, chemical reactions, sublimation, attrition of particles in moving-bed or fluidization reactors [4]). Some of the situations mentioned above had already been investigated in fairly general terms, e.g. fluidization reactors [5], or crystallization [12].

The main object of this paper is to predict the behaviour of a system depicted qualitatively in Fig. 1.

At time $t = 0$, the particle size distribution is characterized with the corresponding initial size frequency curve p_0. The mechanism of mass transfer from solid particles into the solvent results in decreasing the mass of the solid phase as a function of time. The

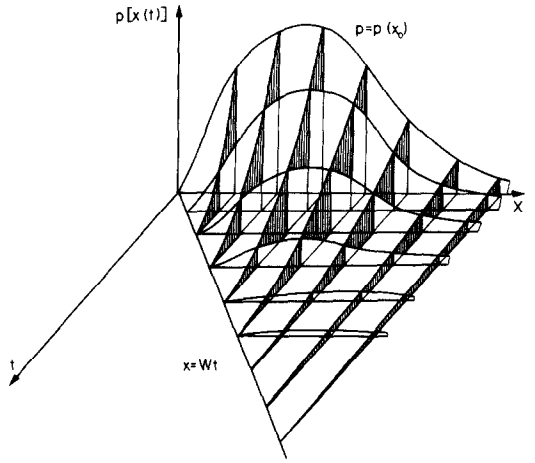

FIG. 1. Time dependency of the size frequency curve in dissolving a polydisperse mixture of solid particles.

particle size decreases and particular fractions gradually disappear. It is assumed that, during the process, no solid particles are entering or leaving the system nor are new particles generated within the system. An example of situation for which the above mentioned features are typical is batch dissolution of polydisperse mixtures of solid particles in a mechanically agitated liquid.

2. THEORETICAL MODEL

Particle size distribution

Particle size distribution analyses are carried out experimentally. Among the commonly used experimental methods, screening is the most frequently employed procedure. Results of a screening analysis are usually expressed in terms of the cummulative oversize (residue) curve R, giving the mass-fraction of particles greater than size x. On the other hand, the size frequency relation p, being a more illustrative description of the size distribution, gives the mass fraction of particles within the size interval x to $x+\mathrm{d}x$. Both quantities are interrelated by means of the simple expression,

$$p = -\frac{\mathrm{d}R}{\mathrm{d}x}. \tag{1}$$

Introducing the characteristic dimension x, which is the diameter of a spherical particle of the same mass as the actual nonspherical particle, the particle-mass M_p is expressed as

$$M_p = \frac{\pi}{6}\rho_s x^3. \tag{2}$$

Mass of the differential fraction $M^{(x)}$ consisting of particles in the size interval x to $x+\mathrm{d}x$ then becomes

$$M^{(x)} = Mp\,\mathrm{d}x = -M\,\mathrm{d}R, \tag{3}$$

where M denotes the total mass of the particle mixture.

In order to express the size distribution characteristics p or R analytically, several expressions had been proposed in the past. A very useful and flexible analytical expression has been found by Rosin, Rammler [10, 11] and independently by Sperling. This relation, which is in the literature usually referred to as the RRS-distribution, has the form

$$R = \exp[-(x/\bar{x})^n], \tag{4}$$

or

$$p = \frac{n}{\bar{x}}\left(\frac{x}{\bar{x}}\right)^{n-1}\exp[-(x/\bar{x})^n], \tag{5}$$

where n and $\bar{x}$ are material constants, characterizing the polydisperse mixture under investigation. The mean statistical diameter $\bar{x}$ is a whole measure of the mixture fineness whereas n characterizes the degree of polydispersity. It is worth to note that all the quantities M_p, $M^{(x)}$, p, R as well as x defined above are time-dependent if particle size changes occur during the process.

Mass transfer between the polydisperse mixture and fluid phase

In what follows we shall assume that mass transfer occurs between the particles of the polydisperse system and the surrounding fluid. At time $t = 0$ the polydisperse mixture is characterized with the initial mass $M(t=0) \equiv M_0$ and the corresponding initial cummulative oversize curve $R(t=0) \equiv R_0$, from which the initial size frequency distribution $p(t=0) \equiv p_0$ may easily be established in view of equation (1). Due to the mass transfer between the phases, particle size may increase or decrease in the course of the particular process. From the equation for mass transfer through the interphase boundary we may express the time rate of particle size change in the form

$$\dot{x} \equiv \frac{\mathrm{d}x}{\mathrm{d}t} = \pm W. \tag{6}$$

The quantity W is determined through the particular mechanism of mass transfer and depends mainly on the physical and geometrical parameters of the system. In certain practically important situations, $W = \text{const.}$ For the system defined above, we may determine the number of particles $n_p^{(x)}$ in the differential fraction $M^{(x)}$ characterized with the particle size range x to $x+\mathrm{d}x$. If at the instant t, the corresponding mass of the differential fraction and size frequency distribution are $M^{(x)}$ and p respectively, we have

$$\begin{bmatrix}\text{number of particles in the size range } x \text{ to } x+\mathrm{d}x \text{ at time } t\end{bmatrix} = \begin{bmatrix}\text{mass of differential fraction at time } t\end{bmatrix} \Big/ \begin{bmatrix}\text{mass of a single particle of size } x \text{ at time } t\end{bmatrix} \tag{7}$$

or,

$$n_p^{(x)} = M^{(x)}[x(t)]/M_p = M \cdot p[x(t)]\,\mathrm{d}x/M_p. \tag{8}$$

For $t = 0$, the initial number of particles follows from equation (8),

$$n_{p0}^{(x)} = M^{(x)}[x(0)]/M_{p0} = M_0\, p_0\, \mathrm{d}x/M_{p0}. \tag{9}$$

Since particles falling into the same size range will be generated or disappear simultaneously, their number must not depend on time, i.e.

$$n_p^{(x)} = n_{p0}^{(x)}. \tag{10}$$

Keeping this in mind and assuming that changes of particle size shall not affect their shape, we can express the mass of the differential fraction $M^{(x)}$ from equations (2) and (8)–(10),

$$M^{(x)} = M_0 M_p p_0 \, dx / M_{p0} = M_0 (x/x_0)^3 p_0 \, dx . \quad (11)$$

For a polydisperse mixture with a particle size varying continuously from $x_{0\,min}$ to $x_{0\,max}$ at $t = 0$, the instantaneous total mass is obtained by summing the differential contributions in equation (11), i.e.

$$M/M_0 = \int_{x_{0\,min}}^{x_{0\,max}} (x/x_0)^3 p_0 \, dx . \quad (12)$$

The instantaneous size frequency distribution is obtained from equation (8)–(10) and (12),

$$p(x_0, t) = \frac{M_0}{M} \frac{M_p}{M_{p0}} p_0 = p_0(x) \psi(t), \quad (13)$$

where the multiplicative factor

$$\psi(t) = (x/x_0)^3 \Big/ \int_{x_{0\,min}}^{x_{0\,max}} (x/x_0)^3 p_0 \, dx \quad (14)$$

is a function of time only. From equation (13) it is clear that the size frequency curves will all be similar in subsequent time intervals.

On the other hand, the time rate of change of the solid phase is

$$\dot{M} = \pm \frac{dM}{dt}, \quad (15)$$

where the plus or minus sign refers to situations in which particle mass increases or decreases with time.

Substituting for M from equation (12) into equation (15) we have,

$$\dot{M} = \pm M_0 \frac{d}{dt} \int_{x_{0\,min}}^{x_{0\,max}} (x/x_0)^3 p_0 \, dx = \pm 3 M_0 \int_{x_{0\,min}}^{x_{0\,max}} (x^2 \dot{x}/x_0^3) p_0 \, dx , \quad (16)$$

since the limits of the integral are time-independent.

Dissolution of the polydisperse solid phase

Let us apply the general equations derived above to the particular case of dissolving a solid polydisperse mixture in a stirred fluid. Kinetics of dissolving a differential fraction of particle size x is described with the fundamental transport equation,

$$\dot{M}^{(x)} = -\frac{dM^{(x)}}{dt} = k A^{(x)} \Delta c , \quad (17)$$

where $A^{(x)}$ denotes the surface of the particles within the differential fraction and Δc stands for the driving force of the process. The mass-transfer coefficient k may be determined either experimentally [7, 3], or predicted from existing criterial equations or empirical formulas [6, 3]. We shall assume the mass-transfer coefficient to be constant in the course of dissolution. This assumption will not hold in situations in which dissolution of large quantities of solid solute results in substantial changes of the volumetric concentration in the surrounding fluid solvent. Also, it is assumed that the dependence of the mass-transfer coefficient upon the particle size is insignificant in most cases [6]. The instantaneous value of the driving force is given by the difference of concentrations corresponding to the saturation at the temperature of solvent in the vessel and in the surrounding fluid. In dissolving relatively small quantities of highly soluble solid particles however, the driving force remains essentially constant. We shall make use of this assumption throughout the following analysis. The interphase surface for non-spherical particles of size x may be expressed as

$$A^{(x)} = \frac{\pi}{\sigma} n_p^{(x)} x^2 , \quad (18)$$

where σ denotes particle sphericity.

Substitution for $A^{(x)}$ from equation (17) into (18) yields

$$\dot{M}^{(x)} = -\frac{\pi}{\sigma} k x^2 n_p^{(x)} \Delta c . \quad (19)$$

If, on the other hand, the L.H.S. of equation (19) is expressed by differentiating equation (11) with respect to time and subsequently use is made of equations (2) and (8), elimination of the particle number $n_p^{(x)}$ gives the value of W in equation (6),

$$\dot{x} = -\frac{2k \Delta c}{\sigma \rho_s} = -W . \quad (20)$$

Integrating equation (20) with the initial condition $x(t = 0) \equiv x_0$ yields a linear relationship for the particle size decrease

$$x = x_0 \left(1 - \frac{Wt}{x_0}\right). \quad (21)$$

In the course of the dissolution process, particular fractions gradually disappear. From equation (21) it is not difficult to deduce that at time t fraction with the initial particle size

$$x_0 = Wt , \quad (22)$$

must disappear, see Fig. 1. Substituting from equations (21) and (22) into the more general equation (12) yields the mass of the solvent as a function of time, i.e.

$$M/M_0 = \int_{Wt}^{x_{0\,max}} \left(1 - \frac{Wt}{x_0}\right)^3 p_0 \, dx . \quad (23)$$

Similarly, an expression for the rate of mass transfer follows from equations (16), (20) and (21),

$$\dot{M} = 3 W M_0 \int_{Wt}^{x_{0\,max}} \left(1 - \frac{Wt}{x_0}\right)^2 \frac{1}{x_0} p_0 \, dx . \quad (24)$$

Finally, the instantaneous size frequency distribution p is obtained combining equations (13), (14), (21) and (22),

$$p = \left(1 - \frac{Wt}{x_0}\right)^3 \Big/ \int_{Wt}^{x_{0\,max}} \left(1 - \frac{Wt}{x_0}\right)^3 p_0 \, dx . \quad (25)$$

In order to specify the quantities in equations (23), (24) and (25) for the particular case of the RRS-distribution given in equation (4), it is convenient to introduce the dimensionless particle size at $t = 0$, i.e.

$$\xi = (x_0/\bar{x}_0)^n . \quad (26)$$

Since from equations (4) and (26),

$$p_0\,\mathrm{d}x = -\mathrm{d}R_0 = \exp[-(x_0/\bar{x}_0)^n]\,\mathrm{d}(x_0/\bar{x}_0)^n = \exp(-\xi)\mathrm{d}\xi,$$

equation (23) turns into

$$M/M_0 = \int_{(Wt/\bar{x}_0)^n}^{\xi_{max}} \left(1 - \frac{Wt}{\bar{x}_0\,\xi^{1/n}}\right)^3 \exp(-\xi)\mathrm{d}\xi. \quad (27)$$

Defining the dimensionless time

$$\vartheta = (Wt/\bar{x}_0)^n, \quad (28)$$

where the bracketed term is the ratio of the real time to the time necessary for completing the dissolution of particles of mean statistical size $\bar{x}_0$ and keeping in mind that the RRS distribution assumes a span of particle size from zero to infinity, equation (27) is rewritten into the form

$$M/M_0 = \int_{\vartheta}^{\infty} [1-(\vartheta/\xi)^{1/n}]^3 \exp(-\xi)\mathrm{d}\xi. \quad (29)$$

Though theoretically correct, equation (29) is impractical since it predicts infinitely long dissolution times. In order to circumvent this difficulty however, we can assume the maximum particle size to be that for which the value of the corresponding cummulative oversize function is $R = 0.001$ [10, 11]. Making use of equation (4), the maximum particle size thus becomes

$$x_{0\,max} = (3\ln 10)^{1/n}\bar{x}_0 = 6.91^{1/n}\bar{x}_0. \quad (30)$$

Under this assumption, the upper limit of the integral in equation (27) attains a finite value $\xi_{max} = 6.91$ and the total time of complete dissolution is correctly predicted as $t_{max} = x_{0\,max}/W$. Therefore, it seems to be reasonable to normalize both variables defined in equations (26) and (28) with respect to ξ_{max}, i.e.

$$\tau = \vartheta/6.91; \quad \eta = \xi/6.91. \quad (30, 31)$$

In terms of the newly defined variables, equation (27) turns into the form

$$M/M_0 = 6.91\int_{\tau}^{1} [1-(\tau/\eta)^{1/n}]^3 \exp(-6.91\eta)\mathrm{d}\eta. \quad (32)$$

Since τ as well as η vary in the interval $\langle 0\text{–}1\rangle$ the latter form is more convenient for computational purposes.

In a similar way, the time rate of mass transfer in equation (24) alternatively becomes

$$\dot{M} = \frac{3WM_0}{\bar{x}_0}\int_{\vartheta}^{\infty} [1-(\vartheta/\xi)^{1/n}]^2 \xi^{-1/n}\exp(-\xi)\mathrm{d}\xi, \quad (33)$$

or

$$\dot{M} = 6.91^{1-1/n}\frac{3WM_0}{\bar{x}_0}\int_{\tau}^{1} [1-(\tau/\eta)^{1/n}]^2 \times \eta^{-1/n}\exp(-6.91\eta)\mathrm{d}\eta. \quad (34)$$

If necessary, the instantaneous size frequency distribution is obtained transforming equation (25) with either ξ, ϑ or τ, η.

Numerical values of $M/M_0 = f(\tau)$ and

$$\dot{M}\bar{x}_0/(3M_0W) = \varphi(\tau)$$

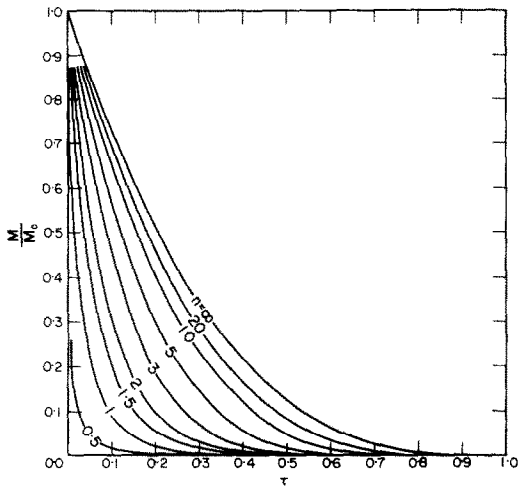

FIG. 2. Variation of the polydisperse solute mass with time.

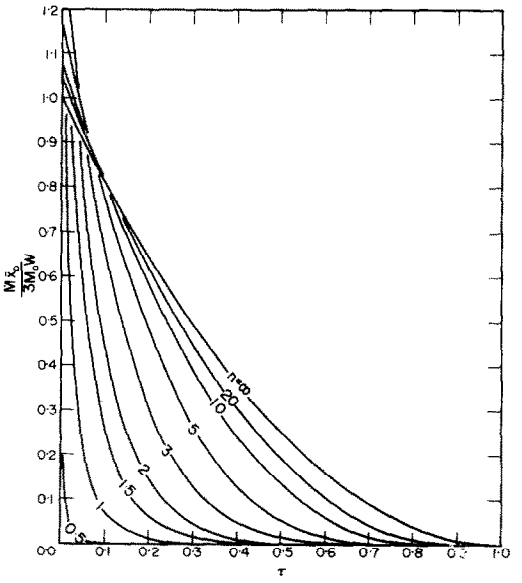

FIG. 3. Time rate of mass transfer vs time.

were obtained by numerical integration of equations (32) and (34) on a digital computer. For some values of the polydispersity index n, results of the numerical analysis are shown graphically in Figs. 2 and 3. Large scale diagrams showing a finer subdivision of the n-range are available on the author's address and will be sent on request. It is worth to note that all the integrals occuring in equations (29), (32), (33) and (34) are expressible in terms of the incomplete gamma-function $\Gamma(\vartheta, m)$ [1],

$$\Gamma(\vartheta, m) = \Gamma(0, m)[1 - I(\vartheta, m)] = \int_{\vartheta}^{\infty} \xi^{m-1}\exp(-\xi)\mathrm{d}\xi, \quad (35)$$

where

$$\Gamma(0, m) = \Gamma(m),$$

and

$$I(\vartheta, m) = \frac{1}{\Gamma(m)}\int_{0}^{\vartheta} \xi^{m-1}\exp(-\xi)\mathrm{d}\xi. \quad (36)$$

Using the tables of Pagurova [8], where highly accurate values of the $I(\vartheta, m)$-function are given, results of the numerical integration were checked for selected values of ϑ and n disclosing a relative deviation not exceeding 1.5%.

3. EXPERIMENTAL APPARATUS AND PROCEDURE

The measurements were carried out on an apparatus which is shown schematically in Fig. 4. Agitator shaft rotation was derived from a hydraulic power unit. The rotational speed was accurately indicated by means of a photoelectric pickup attached to a frequency counter. The geometrical arrangement of the vessel and agitator impeller is shown in Fig. 5.

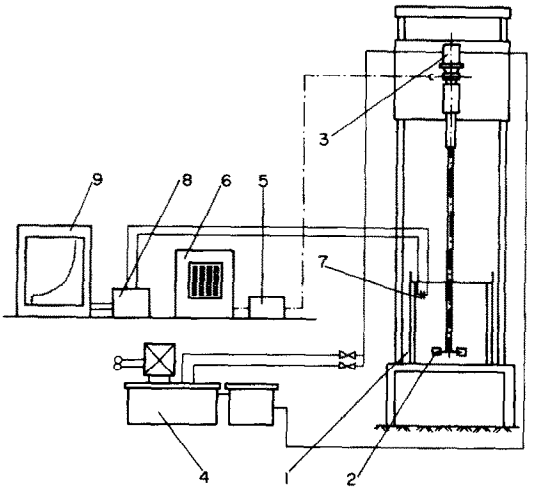

FIG. 4. The experimental apparatus. 1—Vessel, 2—impeller, 3—hydraulic drive, 4—hydraulic power unit, 5—photoelectric pickup, 6—frequency counter, 7—conductometric probe, 8—measuring bridge, 9—line recorder.

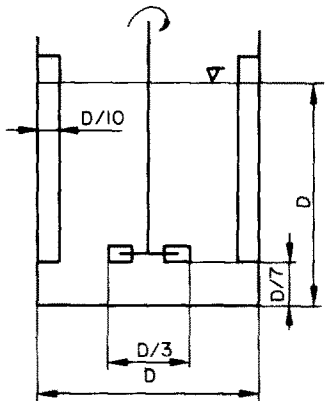

FIG. 5. Details of the impeller and vessel arrangement.

A flat bottom, cylindrical vessel with four baffles was used. The inner diameter of the vessel was $D = 0.2$ m. The turbine impeller was operated at 600 rev/min in all experimental runs. This rotational speed proved to be well above the minimum value necessary to keep the particles in a state of complete suspension. All the measurements were carried out at a constant temperature of 25°C. This was achieved by mounting a jacket around the vessel and circulating water from a thermostat into the gap.

Variation of the solute concentration was measured employing the conductometric method [3]. Output signals from the measuring bridge, which were proportional to the instantaneous solute concentration, were fed to the input terminals of a line-recorder.

As a model material, almost spherical particles of crystalline potassium sulfate K_2SO_4 were used. On a set of laboratory screens, the original granular material was separated into 21 fractions. These in turn were weighed and combined such as to give 24 samples with 12 different combinations of the characteristic $\bar{x}_0$ and n-parameters. In the first 12 samples the maximum particle size was held at the constant value $x_{0\,max} = 1.5$ mm and the polydispersity index attained the values $m = 1$; 1.25; 1.75; 5; 10; 50. In the remaining 12 samples, the mean statistical particle size was held constant $\bar{x}_0 = 0.232$ mm, the polydispersity index attained the same values as above.

The concentration of the saturated K_2SO_4-solution in distilled water at 25°C is $c_s = 120\,\mathrm{kgm^{-3}}$. The average concentration in the course of measurement being $c = 5.11\,\mathrm{kgm^{-3}}$, the average value of the driving force was $\Delta c = 114.89\,\mathrm{kgm^{-3}}$. From the recorded course of the dissolution curve of a monodisperse mixture, $x_0 = 0.232$ mm, the value of $W = 1.257 \times 10^{-5}\,\mathrm{ms^{-1}}$ was obtained employing a linearization procedure. Details of the procedure are given elsewhere [9]. For spherical particles $\sigma = 1$, K_2SO_4 density $\rho_s = 2660\,\mathrm{kgm^{-3}}$, the average value of the mass-transfer coefficient was experimentally determined from equation (20) to be $k = 1.455 \times 10^{-4}\,\mathrm{ms^{-1}}$, for a monodisperse sample.

4. EXPERIMENTAL RESULTS AND CONCLUDING REMARKS

Primary experimental data of the instantaneous solvent concentration $1 - M/M_0$ and time t obtained from the line-recorder were brought into dimensionless form and plotted as M/M_0 vs τ. Typical examples of the experimental results are shown in Figs. 6 and 7.

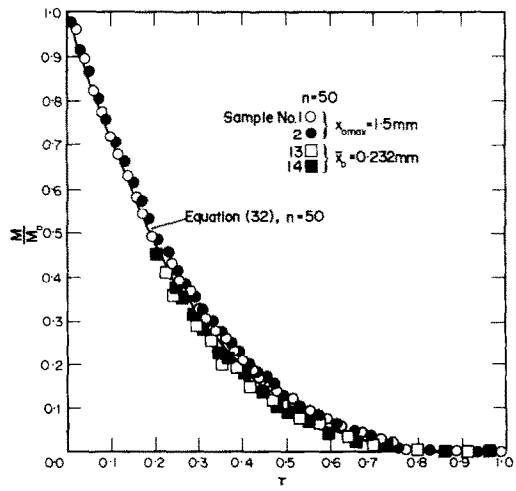

FIG. 6. Variation of the polydisperse solute mass with time, $n = 50$.

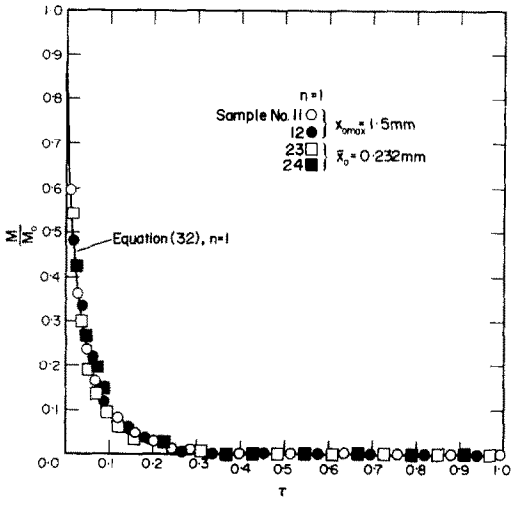

FIG. 7. Variation of the polydisperse solute mass with time, $n = 1.0$.

In Fig. 6, the experimental data for $n = 50$, i.e. for a practically monodisperse mixture are compared with the theoretical prediction embodied in equation (32). Figure 7 presents the same comparison for the other extreme value of the polydispersity index, i.e. for $n = 1.0$ which characterizes a highly polydisperse mixture. From Figs. 6 and 7 it is clear that the agreement between theory and experiment is very good. In fact, relative deviation was always less than 6%.

Since the experimental data support the predictions of the theoretical model, several conclusions may be drawn from what has been derived so far. First of all, it is clear from Figs. 2, 6 and 7 that complete dissolution is reached more rapidly with lower values of the polydispersity index n. In other words, the more polydisperse behaviour the mixture exhibits, the faster is the complete dissolution approached.

These conclusions are in accordance with the predictions of the time rate of mass transfer given in equations (33), (34) as well as in Fig. 3. It is not difficult to calculate, e.g. the initial values of the time rate of mass transfer from equation (33),

$$\dot{M}(\vartheta = 0) = \frac{3WM_0}{\bar{x}_0}\int_0^\infty \xi^{-1/n}\exp(-\xi)\,d\xi = \frac{3WM_0}{\bar{x}_0}\Gamma\left(1-\frac{1}{n}\right). \quad (37)$$

For $n = 1.0$ this expression yields an infinite initial rate of mass transfer which is very closely approximated by the experimental findings shown in Fig. 7. On the other hand, for a monodisperse mixture for which $\bar{x}_0 \equiv x_0$ and $n = \infty$ theoretically, equation (37) predicts

$$\dot{M}(\vartheta = 0, n \to \infty) = 3WM_0/x_0, \quad (38)$$

as expected.

Obviously, many of the polydisperse mixtures encountered in practical applications cannot be described by a single RRS-distribution, i.e. with only two characteristic parameters, $\bar{x}_0$ and n. These situations may also be handled with the general technique outlined in this paper since all the theoretical results up to equation (25) are valid regardless of the particular form of the size frequency distribution. Thus it is always possible to divide the particle size range into smaller intervals in which the RRS-distribution is expected to hold. If necessary, any other size frequency distribution such as, e.g. the normal or logarithmic distribution may be substituted for p_0 into the general equations and integrated numerically or analytically, if possible. As noted earlier, the analysis assumes the driving force to remain constant. This in turn restricts the applicability of the theory to situations in which dilute solutions are formed during the dissolution process.

REFERENCES

1. H. Bateman and A. Erdélyi, *Higher Transcendental Functions*, Vol. 2, p. 133. McGraw-Hill, New York (1953).
2. H. W. Cremer and T. Davies, *Chemical Engineering Practice*, Vol. 3, pp. 2–47. London (1956).
3. P. Ditl, Dissolution mass transfer, Ph.D. Thesis, ČVUT-Faculty of Mechanical Engineering, Prague (1973) (In Czech).
4. D. Kunii and O. Levenspiel, *Fluidization Engineering*, pp. 335–349. John Wiley, New York (1969).
5. O. Levenspiel, D. Kunii and T. Fitzgerald, The processing of solids of changing size in bubbling fluidized beds, *Powder Technol.* **2**, 87–96 (1968/69).
6. D. M. Levins and J. R. Glastonbury, Particle–liquid hydrodynamics and mass transfer in a stirred vessel, Part II. Mass Transfer, *Trans. Instn Chem. Engrs* **50**, 132–146 (1972).
7. S. Nagata, I. Yamaguchi, S. Yaguta and M. Harada, Mass transfer in agitated liquid–solid systems, *Mem. Fac. Engng Kyoto Univ.*, Part I, **22**, 86–122 (1960).
8. V. I. Pagurova, Tables of the incomplete gamma function, Computational Centre of the Soviet Academy of Science, Moscow (1963) (In Russian).
9. K. Partyk, Mass transfer from a polydisperse solid phase into an agitated liquid, M.Sc. Thesis, ČVUT-Faculty of Mechanical Engineering, Prague (1974) (In Czech).
10. E. Rammler, Gesetzmässigkeiten in der Kornverteilung zerkleinerter Stoffe, *Z. Ver. Dt. Ing.* 161–168 (1937).
11. E. Rammler, Zur Ermittlung der spezifischen Oberfläche des Mahlgutes, *Z. Ver. Dt. Ing.* 1950–1960 (1940).
12. A. D. Randolph, The mixed suspension, mixed product removal crystallizer as a concept in crystallizer design, *A.I. Ch. E. Jl* **11**, 424–430 (1965).
13. K. Rietema, Heterogeneous reactions in the liquid phase: influence of residence time distribution and interaction in the dispersed phase, *Chem. Engng Sci.* **8**, 103–112 (1958).

CINETIQUE DU TRANSFERT DE MASSE DANS LA DISSOLUTION DE MATERIAUX SOLIDES POLYDISPERSES

Résumé—Un modèle théorique a été développé pour la dissolution de mélanges polydispersés de particules solides dans des liquides agités mécaniquement. Les résultats de l'analyse théorique sont présentés à l'aide d'expressions dans lesquelles la masse du dissolvant solide, le flux de transfert massique et la distribution

de la taille des particules dépendent explicitement du temps. Les équations générales données dans l'article sont valables indépendamment de toute forme particulière de la fonction de distribution en tailles de particules. A titre d'exemple, les équations générales sont intégrées dans le cas particulier de la distribution de Rosin, Rammler et Sperling (RRS). Les résultats de l'analyse sont présentés sous forme de relations graphiques entre quantités adimensionnelles. Afin de vérifier les résultats obtenus par voie théorique, on a effectué des expériences de dissolution de mélanges polydispersés de particules de sulfate de potassium dans l'eau distillée. Un très bon accord entre théorie et expérience a été obtenu.

KINETIK DES STOFFÜBERGANGS BEI DER AUFLÖSUNG VON POLYDISPERSEN FESTSTOFFEN

Zusammenfassung—Für die Auflösung von polydispersen Gemischen aus Festpartikeln in mechanisch gerührten Flüssigkeiten wurde ein theoretisches Modell entwickelt. Die Ergebnisse der theoretischen Analyse werden in Ausdrücken wiedergegeben, in welchen die Masse des festen Stoffes, die Geschwindigkeit des Massenübergangs und die Verteilung der Partikelgröße explicit von der Zeit abhängen. Die in der Arbeit angegebenen allgemeinen Gleichungen gelten unabhängig von der speziellen Form der Funktion der Größenverteilung. Als Beispiel sind die allgemeinen Gleichungen integriert für den speziellen Fall der Rosin, Rammler, Sperling (RRS) Verteilung. Die Ergebnisse der Analyse sind in Diagrammen mit dimensionslosen Parametern wiedergegeben. Zur Bestätigung der theoretisch erhaltenen Resultate wurden Experimente durchgeführt, wobei sich polydisperse Gemische aus Kaliumsulfatteilchen in destilliertem Wasser auflösten. Sehr gute Übereinstimmung zwischen Theorie und Untersuchung ergab sich dabei.

КИНЕТИКА МАССООБМЕНА В РАСТВОРЯЮЩИХСЯ ПОЛИДИСПЕРСНЫХ МАТЕРИАЛАХ

Аннотация — Разработана теоретическая модель для растворения полидисперсных смесей твердых частиц в механически перемешиваемых жидкостях. Результаты теоретического анализа представлены в виде выражений, в которых масса твердой фазы, скорость массообмена и распределение частиц по размерам зависят от времени. Общие уравнения, приведенные в докладе, сохраняют силу безотносительно к виду функции распределения частиц по размерам. В качестве примера, проинтегрированы общие уравнения для случая распределения по Розину, Раммлеру и Сперлингу (РРС). Результаты анализа представлены в виде графических соотношений безразмерных величин. Для проверки результатов, полученных теоретическим способом, проводились эксперименты по растворению полидисперсных смесей частиц сернокислого калия в дистилированной воде. Наблюдалось очень хорошее согласие между теорией и экспериментом.